Chemical and Biological Technologies in Agriculture

Spectroscopic analysis of mushrooms by surface-enhanced Raman scattering (SERS)

Federico Puliga[1*], Veronica Zuffi[1], Alessandra Zambonelli[1], Ornella Francioso[1] and Santiago Sanchez-Cortes[2]

Abstract

Background: Mushrooms have always been considered an important source of food and biologically active compounds with several medicinal properties. In recent years, different methods were used to study the quality and chemical composition of mushrooms. Among these, Fourier transform infrared (FT-IR) and FT-Raman spectroscopy techniques have been successfully applied to identify different mushroom species. However, the structural biomolecule components existing in the mycelium or in the fruiting bodies may produce strong fluorescence emission that overlaps the Raman radiation, thus avoiding their analyses by Raman. SERS spectroscopy is a powerful technique which uses metal nanoparticles (NPs) to enhance the Raman signal of molecules adsorbed on the NPs surface. In addition, SERS is able to quench the macromolecule florescence. In this work, we have employed silver nanoparticles in order to get mushroom fingerprints based on SERS as quick procedure to analyze and identify different chemical compounds from the fruiting bodies of six edible and/or medicinal mushrooms: *Lentinula edodes*, *Ganoderma lucidum*, *Pleurotus cornucopiae*, *Pleurotus ostreatus*, *Tuber aestivum* and *Tuber magnatum*.

Results: SERS analyses performed directly on fruiting body fragments produced characteristic spectra for each species. One group of mushrooms (*L. edodes*, *G. lucidum*, *T. aestivum* and *T. magnatum*) was dominated by the bands of nucleic acids; and the other one (*P. cornucopiae* and *P. ostreatus*), by the bands of pigments such as melanins; carotenoids; azafilones; polyketides; and flavonoids located in the cell wall. Additionally, bands corresponding to cell wall polysaccharides, particularly chitosan and 1,3-β D-glucan, were identified in the extracts of *P. cornucopiae*, *P. ostreatus* and *L. edodes*. No signal of cell wall polysaccharides was found in *G. lucidum* extract. Raman mapping of the analyzed samples was useful in tracking the spatial distribution of the marker bands. Moreover, the principal component analysis (PCA) carried out on the acquired SERS spectra, allows to discriminate the analyzed mushroom species.

Conclusions: The SERS technique has the ability to generate a strong Raman signal from mushroom fruiting bodies using Ag-NPs deposited directly on intact, untreated mushroom tissues. Using this methodology, commonly applied laboratory time-consuming methods can be avoided or bypassed as well as analysis time can be reduced.

Keywords: FT-Raman, SERS spectra, PCA, Ag-NPs, Mushroom identification

*Correspondence: federico.puliga2@unibo.it

[1] Department of Agricultural and Food Sciences, University of Bologna, Viale G. Fanin 40-50, 40127 Bologna, Italy
Full list of author information is available at the end of the article

Puliga *et al. Chem. Biol. Technol. Agric.*   (2022) 9:100

Page 2 of 10

Graphical Abstract
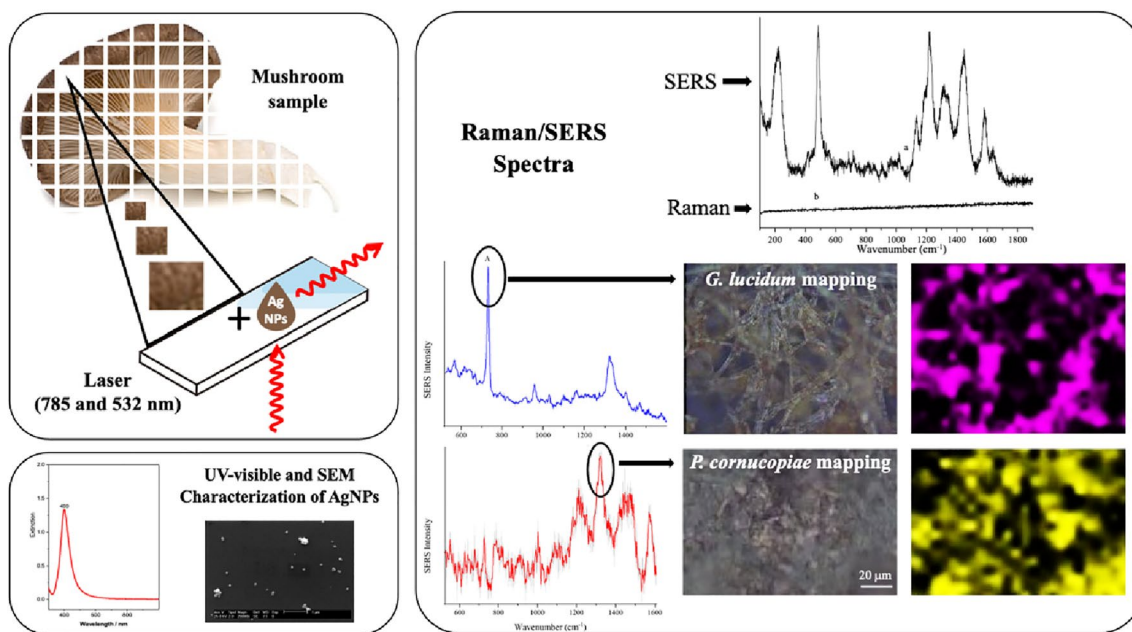
Introduction

Fungi are a kingdom of unicellular or multicellular eukaryotic organisms which has recently been estimated to include up 12 millions of species [1]. Most of them are free-living in soil or water as saprotroph; others establish parasitic or symbiotic relationships with plants or animals. Depending on their aspects, they can be empirically divided in yeasts, filamentous molds, and mushrooms. In particular, mushrooms are defined as the fungi that form a distinctive fruiting body which can be either hypogeous or epigeous, large enough to be seen with the naked eye and to be picked by hand [2, 3]. Mushrooms have always been considered an important source of food and biologically active compounds with several medicinal properties [4]. Traditionally, characterization of fungi has been based on phenotypic characteristics or molecular analysis. However, most of the described fungal species (about 70%) have not yet been sequenced [5]. All these issues reduce the authenticity of the data and the reliability of the analysis. In addition, another concern relates to the time required for analysis, which is both time-consuming and often very expensive.

In recent years, vibrational spectroscopy techniques allow a range of qualitative or quantitative information to be obtained, representing a new frontier for fungal identification [6], as well as Fourier transform infrared spectroscopy (FT-IR) and FT-Raman techniques have been successfully applied to identify different fungal species (*Boletus* spp., *Ganoderma* spp., *Agaricus bisporus* (J.E. Lange) Imbach, *Mucor rouxii* (Calmette) Wehmer and *Mortierella* sp.) [7–9]. However, FT-Raman analysis of biological materials can produce a weak signal, which is often covered by the large fluorescence emitted by the sample after excitation [10]. Likewise, FT-IR analysis of biological materials can produce low-quality spectra due to different tissue hydration. As a result, this may lead to an information loss in the amide region caused by the broad adsorption of water molecules at around 1640 cm^{-1} [11].

Surface-enhanced Raman scattering (SERS), thanks to the use of nanostructured metals (Au and Ag), allows to overcome the intrinsic weakness of Raman spectroscopy combining high molecular specificity with a high sensitivity [12, 13]. The signal enhancement strongly depends on the nanoparticles (NPs) optical properties (i.e., composition, size, and shape), the laser excitation characteristics, the nature of the molecule and its Raman cross-sections [14, 15]. When incident light interacts with the NPs, a localized electric field is generated producing a localized surface plasmonic resonance (LSPR) that allows a strong increase in the Raman scattering up to 10^{14} orders of magnitude compared to the normal Raman technique [16, 17]. Thus, only molecules

Puliga *et al. Chem. Biol. Technol. Agric.* (2022) 9:100

Page 3 of 10

adsorbed or located near the plasmonic substrate produce noticeable amplification of the Raman signal [18, 19]. Moreover, the maximum intensification of the signal occurs at the tips of protruding elements and, even more, in the interparticle nanoscale spaces called "hot spots" [20]. These "hot spots" result from plasmonic coupling between NPs and increase rapidly as the interparticle distance becomes shorter [21]. As a result of their efficacy the SERS-based metallic NPs have been used to characterize complex biological samples such as nucleic acids [22–24] and proteins [25–27] as well as for the study of different microorganisms, including fungi [28–32], yeasts [33], and plant pathogens [34, 35]. Moreover, SERS spectroscopy coupled with the PCA has been employed by several authors to discriminate different fungal species on the basis of their spectra [30, 31, 34].

In the present work we have analyzed six different mushroom species having a high economical interest: *Lentinula edodes* (Berk.) Pegler, *Ganoderma lucidum* (Curtis) P. Karst., *Pleurotus cornucopiae* (Paulet) Rolland, *Pleurotus ostreatus* (Jacq.) P. Kumm, *Tuber magnatum* Picco and *Tuber aestivum* Vittad. The basidiomycetes *L. edodes*, *G. lucidum*, *P. cornucopiae* and *P. ostreatus* are between the most popular and cultivated mushrooms in the world [36, 37]. On the other hand, *T. magnatum* and *T. aestivum* are two truffles (hypogeous ascomycetes into the genus *Tuber*) which are ones of the most highly prized food [38]. Accordingly, the main objective of this work was to develop a fast and simple method for identifying mushrooms with no chemical processing. In addition, in situ analysis of tiny mushroom parts is likely to be a low-cost winning procedure for the characterization of different edible and medicinal mushrooms by SERS spectroscopy combined with chemometric analysis.

Materials and methods
Mushroom samples and conservation
The fruiting bodies of *G. lucidum* (Glu), *L. edodes* (Led), *P. cornucopiae* (Pco), *P. ostreatus* (Pos), *T. aestivum* (Tae) and *T. magnatum* (Tmg) were analyzed. The fruiting bodies of *G. lucidum*, *L. edodes*, *P. cornucopiae* and *P. ostreatus* were obtained through cultivation on sterilized substrates as described in previous works [39, 40]. Samples of *T. aestivum* (herbarium No. 5259) and *T. magnatum* (herbarium No. 3956) were collected in the wild in the provinces of Bologna and Ferrara, Italy, respectively, and stored in the CMI-Unibo Herbarium at the University of Bologna. All samples were dried at 40 °C for 24 h and stored in a desiccator until used.

Raw polysaccharide extraction
Polysaccharide extraction was carried out on 1 g of dried and powdered Glu, Led, Pco and Pos fruiting bodies, following the protocols described by Ma et al. (2014) [41]. The powder was initially treated overnight by immersing it in an 85% ethanol solution. Samples were then centrifuged at $4500 \times g$ for 15 min and the precipitate was extracted in distilled water (25 mL for each g of precipitate) at 70 °C for 140 min. The solution obtained was filtered and centrifuged for 10 min at $4500 \times g$. The supernatant was deproteinized with Sevag reagent (butanol:chloroform, 1:4 v/v) and centrifuged at $4500 \times g$ for 10 min. The upper layer was removed and mixed with four-fold volume of absolute ethanol in order to precipitate the crude polysaccharides for 12 h at 4 °C. Crude polysaccharides were centrifuged at $4500 \times g$ for 15 min and the precipitate was washed with ethanol and acetone and lyophilized.

Chemical reagents
Silver nitrate, trisodium citrate dihydrate, hydroxylamine hydrochloride and other reagents were of analytical grade and purchased from Sigma-Aldrich. All solutions were freshly prepared with Milli-Q® ultrapure distilled water before experiments and used immediately.

Silver NPs preparation
Before silver NPs preparation all glassware was cleaned with aqua regia and rinsed with Milli-Q® ultrapure distilled water to remove any impurities present on glass surface. Solutions of silver nitrate (10^{-2} M) and of hydroxylamine hydrochloride (1.67×10^{-3} M) containing 3.33×10^{-3} M sodium hydroxide were used for silver colloid preparation as described by Leopold and Lendl (2003) [42]. Briefly, 10 mL of silver nitrate solution was added dropwise while stirring to 90 mL the hydroxylamine hydrochloride/sodium hydroxide solution. After preparation the colloidal solution was stored at 4 °C in darkness.

Sampling for SERS spectroscopy and mapping
For SERS analyses, small fragments (3×3 mm) from the cap and pileus of dry fruiting bodies of Led, Glu, Pco and Pos and fragments from the sterile tissue of the gleba of the two *Tuber* species, were placed for 24 h into a 1.5-mL microcentrifuge tube containing 1 mL of Milli-Q® ultrapure distilled water. After 24 h the tubes were centrifuged at $11,000 \times G$ for 10 min and all the water was removed. The small wet fragments of each mushroom species were placed on a microscope slide glass and covered with 5 µL of a concentrated Ag-NPs suspension obtained by centrifugation of 500 µL and successive redispersion to 10% of the original volume. Samples were

Puliga *et al. Chem. Biol. Technol. Agric.*   (2022) 9:100

Page 4 of 10

dried at room temperature before SERS analyses. For each mushroom species three biological replicates were made.

Instrumentation

The silver NPs were characterized by using an UV–VIS spectrophotometer (UV-3600, Shimadzu, Japan). Raman, SERS, and mapping were performed by using the portable spectrometer Renishaw Raman Virsa™ with a 785 and 532 nm lasers. Before measurements a calibration was performed by using a Si reference sample. Mushroom fragments were analyzed under a $50\times$ objective long focal lens and the laser power was set at 2 mW with an integration time of 1 s. Samples were mapped by recording the spectra of an area of around 40×40 µm for a total of 800 spectra for each sample. The spectra were acquired using the Renishaw WiRE 5.5 program and processed by the OriginPro 2019 software (OriginLabs). The SEM picture was obtained in an environmental scanning electron microscope, Philips XL30 (Philips, the Netherlands), with a tungsten filament operating in high vacuum mode. The acceleration voltage was 25 kV.
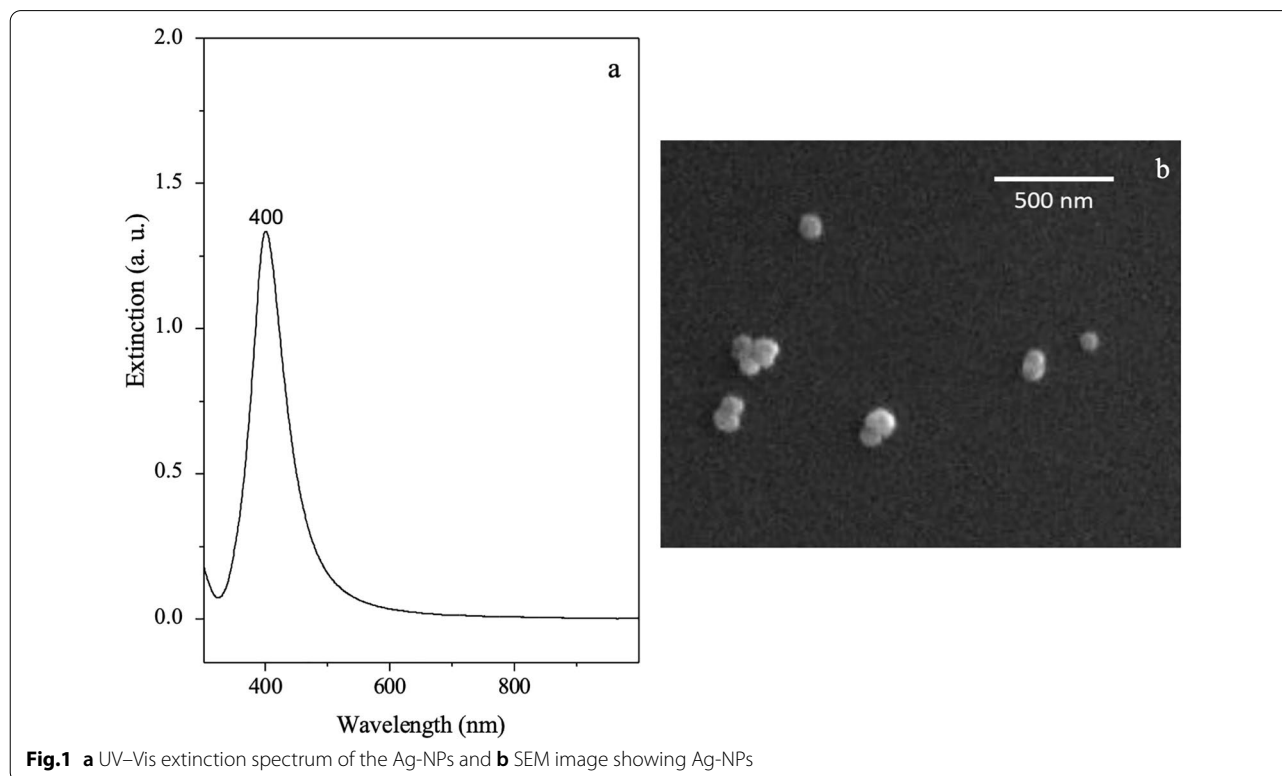
Statistical analysis

Principal component analysis (PCA) was applied to evaluate variations in the data matrix between the analyzed mushrooms in order to identify the single species.
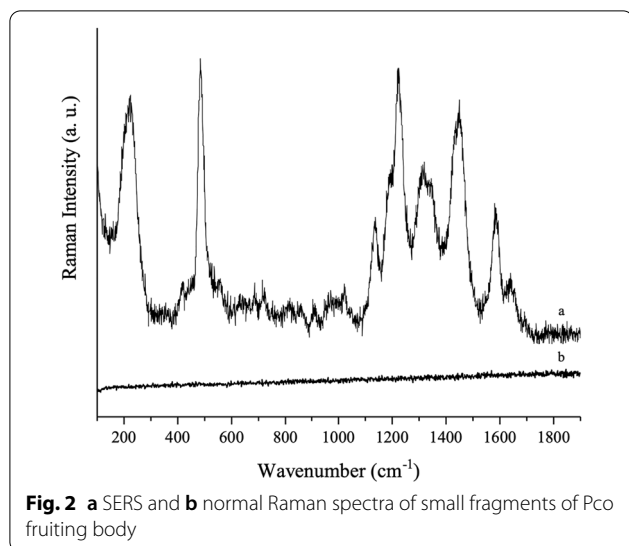
Spectra were previously normalized as reported by Dina et al. [30] on the basis of the vAgX band which represents the most intense peak. Processed spectral data were used because of providing much more accurate information on the sample by solving the bands that were previously overlapped in the raw spectra. The PCA was performed by using the OriginPro software with a matrix having a dimension of 18 samples×2303 variables (wavenumbers units, covering the range 100–1800 cm^{-1}). PCA is performed on the variance–covariance matrix band.

Results and discussion

Ag-NPs characterization

The successful Ag-NPs formation strictly depends on the preparation parameters that can be easily handled to produce Ag-NPs of well-defined shape, structure, and size distribution. Based on previous studies [32, 33, 43] the Ag-NPs formation was confirmed by the presence of a narrow band with an absorption maximum at 400 nm in UV–Vis spectroscopy (Fig. 1a). The higher absorption intensity indicates that the number of Ag-NPs formed in the solution rise with increasing reaction time (Fig. 1a). The nanoparticles produced had an average radius of 40 nm. SEM imaging (Fig. 1b) of Ag-NPs confirmed the particle diameter and spherical shape.


Fig.1 a UV–Vis extinction spectrum of the Ag-NPs and **b** SEM image showing Ag-NPs

Puliga *et al. Chem. Biol. Technol. Agric.* (2022) 9:100

Page 5 of 10

Fig. 2 **a** SERS and **b** normal Raman spectra of small fragments of Pco fruiting body

Fig. 3 SERS spectra of Glu (blue line), Tae (green line), Tmg (orange line), Led (purple line), Pco (red line) and Pos (yellow line). *A* adenine, *G* guanine, *M* melanins, *P* phosphate groups and *T* thymine

Normal Raman and SERS spectroscopy

One of the main objectives of the present work was to characterize the different molecular species present in mushrooms by using the Raman spectroscopy under the specific excitation at 785 nm. The latter excitation wavelength is usually employed in the analysis of biological materials because it leads to a reduced fluorescence. However, the Raman spectra registered at 785 nm produced no vibrational signals (Fig. 2b). Likewise, a broad background fluorescence at 532 nm was detected as a result of pigment molecules excitation within the mushroom cell wall (data not shown). Therefore, normal Raman spectra collected with two different excitation wavelengths were unable to generate spectra from the mushroom samples. By contrast, the direct deposition of a concentrated drop of Ag-NPs on the mushroom surface was sufficient to generate an enhancement of the SERS signal with 785 nm radiation (Fig. 2a). The spectra registered on different points of the analyzed surface revealed few spectral changes between spectra, thus indicating the reproducibility of the analysis (data not shown).

The SERS analyses performed on the six different fungal species (Fig. 3) rendered different spectral responses that can be roughly classified into two main groups. The first one is dominated by nucleic acid signals (adenine (A), guanine (G), thymine (T) and phosphate groups (P)). The second one is characterized by other set of bands that we have assigned to fungal pigments localized in the mushroom cell wall: melanins (M); carotenoids; azaphilones; polyketides, flavonoids, etc. [44]. However, we cannot exclude that these bands are related to the polysaccharides existing in the fungal cell wall as reported by Gieroba et al. (2022) [45]. These two different groups
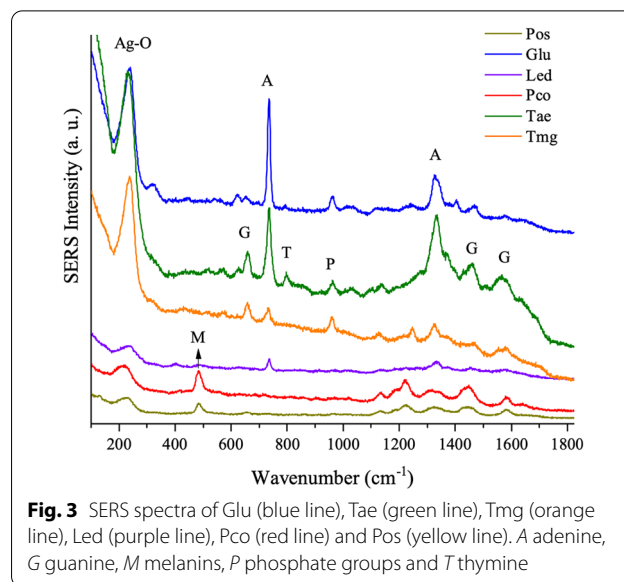
will henceforth be referred to as A-group and B-group, respectively.

In particular, in A-group, the bands of adenine at 735 and 1335 cm^{-1}, and guanine at 660 and 1568 cm^{-1} were clearly visible [46]. The band at 796 cm^{-1} can be assigned to the ring breathing band of cytosine and thymine coupled with phosphate vibrations [46]. Other less intense bands in the 960–1100 cm^{-1} region corresponded to the A-group DNA phosphate and to some ring bands of the purine and pyrimidine bases [22, 46].

The presence of nucleic acid bands in the SERS spectra of fungi was detected in the extracted DNA of *Phytophthora ramorum* Werres, De Cock & Man in 't Veld, and in the analysis of micro-fungi cells [32, 35]. The detection of nucleic material by SERS in the intact non-treated mushroom fragments is an interesting result, because we expected to detect biomolecules localized in the outer part of fungal cell walls. The fact that the fungal genetic material can be put in evidence under the presence of the Ag-NPs implies two possible effects: (a) diffusion of the nanoparticles inside the fungal cells through the wall, and (b) the disruption of the fungal cell wall and the direct interaction of silver with the intracellular material. Both effects are possible and also they were previously described in the literature [47–49].

On the other hand, Ag-NPs have been reported to interact with the fungal membranes through electrostatic interactions [50] or through specific covalent interactions with SH-containing groups leading to the protein denaturation [51]. The latter effect could increase the permeability of the fungal membrane resulting in disruption of the cell membrane [52]. Based on previous studies [50, 52], the appearance of intense bands of nucleic acids

Puliga *et al. Chem. Biol. Technol. Agric.*   (2022) 9:100

Page 6 of 10

(DNA and RNA) in SERS spectra might be due to the disruption of the fungal membrane through the formation of holes in the fungal cell wall and the formation of pores in the plasma membrane through which the cell material can flow outward.

The strong effect of Ag-NPs on DNA and RNA was likely induced by the high affinity of silver for purine and pyrimidine bases. In particular, the interaction of Ag with adenine and guanine has been widely demonstrated in previous SERS analyses of nucleic acids [46, 53]. Our outcomes exhibited changes that may be related to different interaction of DNA and/or possibly RNA with Ag-NPs, as shown in Fig. 3 (Glu, Led, Tae and Tmg). Specifically, the ratio between the ring breathing bands corresponding to adenine (735 cm^{-1}) and guanine (656 cm^{-1}) changed from Glu, where it was maximum and it was dominated by the adenine bands, to Tmg, where the guanine bands were more enhanced in the SERS spectrum. On the other hand, the A/G ratio can be related in SERS with the different hybridization degree of the double-stranded DNA chain [23]. Therefore, in terms of the SERS spectra of mushrooms, this ratio could be related to an effect of silver on the DNA structure.

In the case of B-group (Pos and Pco, Fig. 3), no band corresponding to nucleic acids were observed. Conversely, broad and weak bands were observed at 483, 1223, 1312, 1445 and 1585 cm^{-1}. Similar bands were observed in the case of some pathogenic fungi (*Scopulariopsis brumptii* Salv.-Duval, *Candida krusei* (Castell.) Berkhout, *Trichophyton rubrum* (Castell.) Sabour., *Alternaria alternata* (Fr.) Keissl., *Aspergillus flavus* Link, *Fusarium verticillioides* (Sacc.) Nirenberg, *Aspergillus parasiticus* Speare) previously analyzed by SERS [31, 34]. In addition, these Raman spectra showed a high similarity with the SERS of some of the pigments existing in the fungal cell wall, such as flavonoid pigments [54]. More specifically, bands at 1223, 1312 or 1445 cm^{-1} are visible in fungal melanins that were identified in the fungus *Ochroconis* sp. by SERS [55, 56]. The prevalence of bands corresponding to pigments presumably embedded in the fungal wall indicated that the cell wall of Pos and Pco remained intact in the presence of Ag-NPs. Therefore, the absence of cell wall rupture resulting in the opening of the plasma membrane could be related to its organization. In fact, it is structured in several layers, with the innermost layer consisting of a covalently bound β-(1,3) glucan core and branched chitin [57, 58]. The outer layers, in contrast, are more heterogeneous and adapted to the physiology of particular fungi and generally composed of polysaccharides such as β-(1,6) glucan, mannan, galactomannan, and also highly mannosylated glycoproteins [59]. In addition, pigments such as melanin are found in this outer layer, as was detected in the SERS of

Pco. This peculiar organization of the cell wall provides greater resistance to Ag-NPs.

In addition, another important difference between the mushrooms of the A and B-group is the position of the stretching Ag–X band (vAgX), where X can designate the atom (normally O, S or N) of the fungal biomolecule directly interacting with the metal. This band appeared at 237 cm^{-1} in the case of the A-group mushrooms, while it is shifted to 220 cm^{-1} in the mushrooms of the B-group.
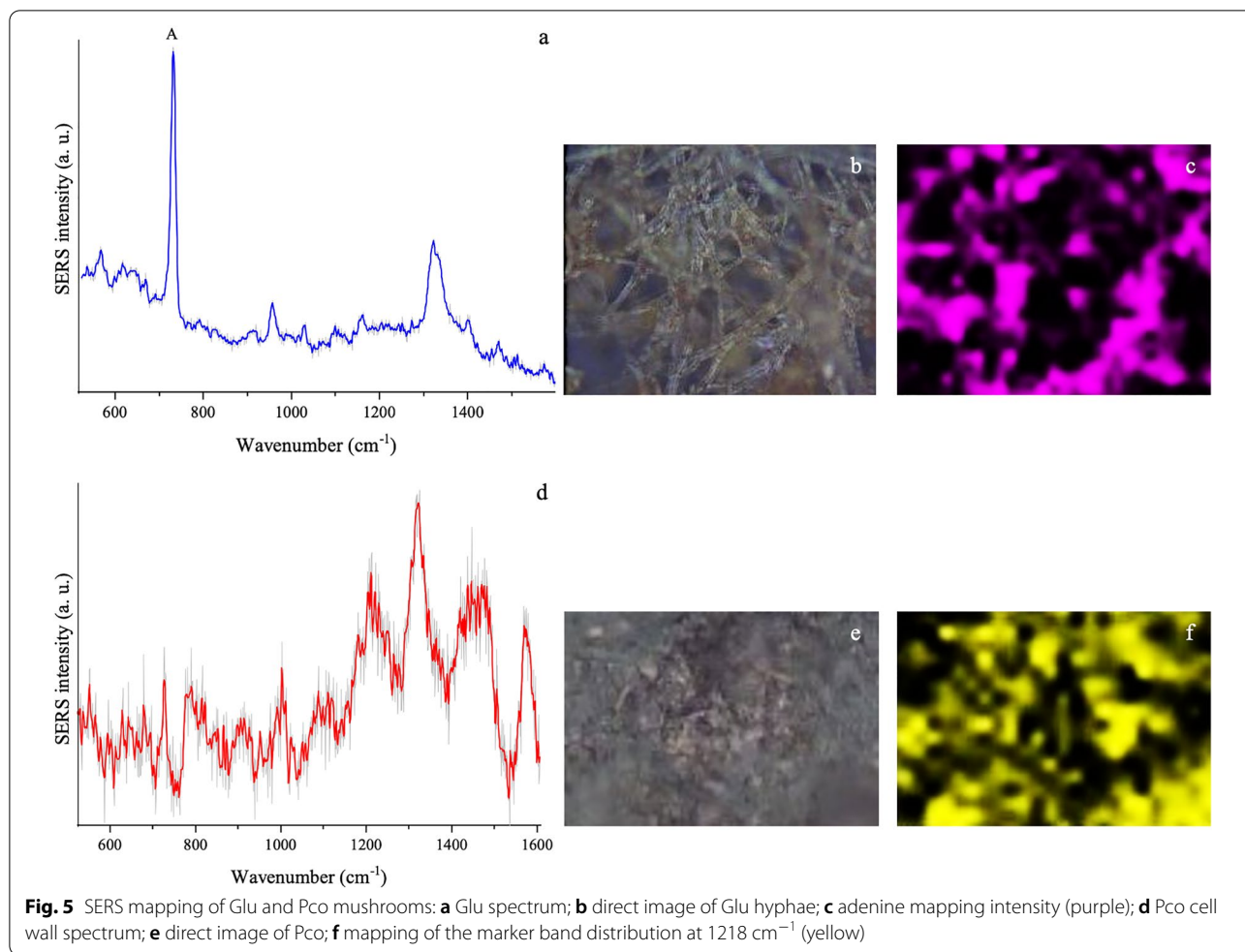
For assessing the origin of the SERS Pco and Pos spectra shown in Fig. 3, polysaccharides from fungi of A-group (Glu and Led) and B-group (Pco and Pos) were investigated.

The SERS spectra of polysaccharides are displayed in Fig. 4. The bands corresponding to the cell wall from 1100 to 1600 cm^{-1} were evident in the Glu, Pos and Pco. However, in the case of Glu (A-group), these bands were not detected in the SERS of intact fruiting body fragments demonstrating the disruption of the cell wall of this mushroom at the presence of Ag-NPs. In the specific case of Led, the adenine bands are still strong in the SERS spectrum of the extracted polysaccharides. This is likely due to the adsorption of Led A-rich DNA sequences to the wall fragments.

Polysaccharides, mainly β-glucans, are particularly important as they are linked to the medicinal properties of mushrooms (e.g., immunomodulatory, anticancer, and antioxidant). In particular, Glu and Led mushrooms are among of the most important medicinal mushrooms cultivated in the world [60].
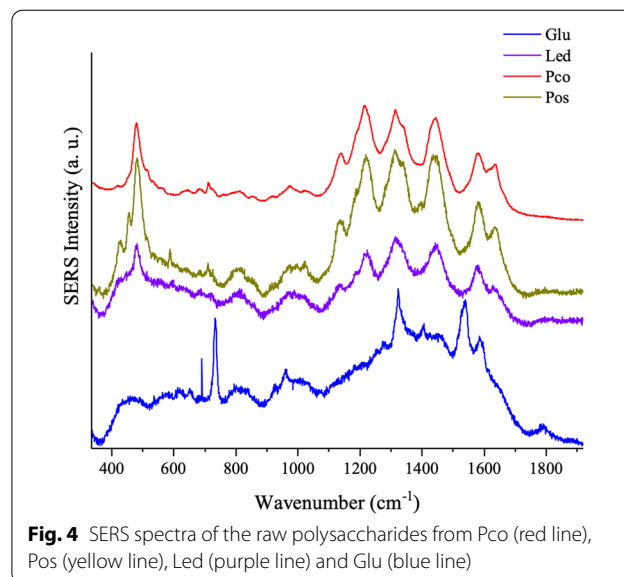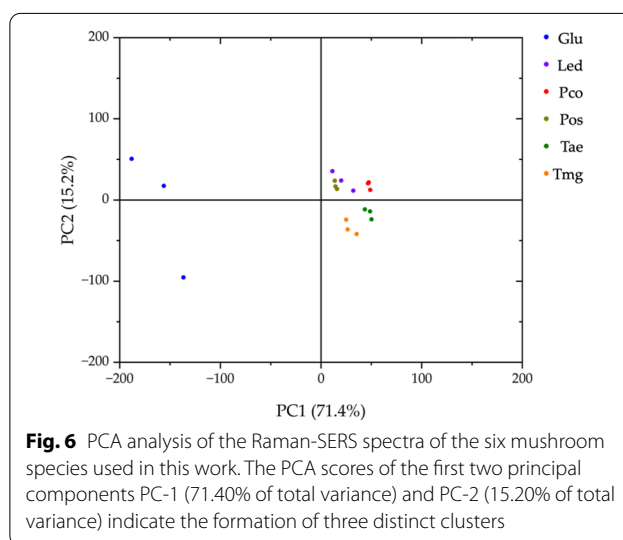

Fig. 4 SERS spectra of the raw polysaccharides from Pco (red line), Pos (yellow line), Led (purple line) and Glu (blue line)

Fig. 5 SERS mapping of Glu and Pco mushrooms: **a** Glu spectrum; **b** direct image of Glu hyphae; **c** adenine mapping intensity (purple); **d** Pco cell wall spectrum; **e** direct image of Pco; **f** mapping of the marker band distribution at 1218 cm^{-1} (yellow)

Raman mapping and PCA analysis

SERS mapping of Glu and Pco (Fig. 5) was carried out in order to investigate the spatial distribution of bands corresponding to nucleic acids and the fungal cell wall pigments. Figure 5b shows the optical direct image of Glu where the hyphae of the fungus are clearly observed. Figure 5c displays the intensity (purple) of the adenine marker band (735 cm^{-1}). An individual spectrum of a certain point is shown for comparison in Fig. 5a. From this mapping it is possible to corroborate that the signal is located in the hyphae. In the case of Pco, the spectrum corresponds to the fungal cell wall (Fig. 5d), as well as the direct image (Fig. 5e) and the mapping of the marker band distribution at 1218 cm^{-1} (Fig. 5f). The distribution maps were also recorded to demonstrate the method reproducibility, since the areas with the most intense spectra exhibited no significant variation in the SERS spectral pattern.

The PCA analysis of the Raman-SERS spectra (100–1800 cm^{-1}) allows to discriminate different mushroom

Fig. 6 PCA analysis of the Raman-SERS spectra of the six mushroom species used in this work. The PCA scores of the first two principal components PC-1 (71.40% of total variance) and PC-2 (15.20% of total variance) indicate the formation of three distinct clusters

species. PC-1 scores accounted for 71% of the total variance of the analyzed dataset, thereby demonstrating separation of the studied mushrooms into three separate clusters (Fig. 6). The first cluster comprises Led, Pco and Pos which belongs to Agaricales order; the second one is represented by Glu species which belong to the Polyporales order. The latter group include Tae and Tmg belonging to Tuberales order.

Conclusions

In conclusion, only the SERS technique can afford significant Raman signals from the analyzed mushrooms by the use of Ag-NPs directly dropped onto the intact non-treated biological tissue of the fruiting bodies. The normal Raman spectroscopy is not able to provide vibrational signals due to the high fluorescence emission. SERS provides a very simple and rapid protocol to identify marker biomolecules of cell wall or the nucleic acid components, that can serve to univocally identify the species. Accordingly, two main groups of mushrooms can be recognized from the SERS data based on different spectral patterns: (a) those dominated by nucleic acid signals; and (b) those dominated to other set of bands that we have assigned to fungal pigments localized in the mushroom cell wall. The pigments identified in the fungal cell wall are of polyphenolic nature and could be related to melanins and flavonoids present in this wall. The polysaccharide bands of the cell walls, particularly chitosan and 1,3-D glucan, were exclusively visible in the Pco and Pos spectra and extremely weak in Led, although these bands are also mixed with those of fungal pigments. Raman mapping of fungi was useful for tracing the spatial distribution of marker bands and getting a large number of spectra from a given area, confirming a high repeatability of the analysis. Additionally, the SERS spectra were processed with the PCA algorithm, and the outcomes revealed that they explained 86.6% of the variance among the data. Based on above, the PCA clearly exhibits its applicability with a limited number of fungal species as well. Thus, by using this methodology, more time-consuming methods commonly applied in the laboratory can be avoided or bypassed as well as analysis time can be reduced.

Abbreviations

SERS: Surface-enhanced Raman scattering; FT-IR: Fourier transform infrared; NPs: Nanoparticles; PCA: Principal component analysis; LSPR: Localized surface plasmonic resonance; Glu: *G. lucidum*; Led: *L. edodes*; Pco: *P. cornucopiae*; Pos: *P. ostreatus*; Tae: *T. aestivum*; Tmg: *T. magnatum*; A: Adenine; G: Guanine; T: Thymine; P: Phosphate groups; M: Melanines; Chi: Chitosan; Glc: Glucan.

Author contributions
Conceptualization, FP and SSC; methodology, FP and SSC; validation, SSC; formal analysis, FP and SSC; investigation, FP and VZ; resources, SSC, AZ and OF; data curation, SSC; writing—original draft preparation, FP; writing—review and editing, FP, VZ, SSC, OF and AZ; visualization, FP, SSC and VZ; supervision, SSC, OF and AZ; funding acquisition, SSC. All authors read and approved the final manuscript.

Availability of data and materials
The datasets used and/or analyzed during the current study are available from the corresponding author on reasonable request.

Declarations

Ethics approval and consent to participate
Not applicable.

Consent for publication
Not applicable.

Competing interests
The authors declare that they have no competing interests.

Author details
[1]Department of Agricultural and Food Sciences, University of Bologna, Viale G. Fanin 40-50, 40127 Bologna, Italy. [2]Instituto de Estructura de La Materia, IEM-CSIC, Serrano, 121, E-28006 Madrid, Spain.

References

1. Wu B, Hussain M, Zhang W, Stadler M, Liu X, Xiang M. Current insights into fungal species diversity and perspective on naming the environmental DNA sequences of fungi. Mycology. 2019. https://doi.org/10.1080/21501203.2019.1614106.
2. Chang ST, Miles PG. Mushroom biology—a new discipline. Mycologist. 1992;6:64–5.
3. Wasser S. Medicinal mushrooms as a source of antitumor and immunomodulating polysaccharides. Appl Microbiol Biotechnol. 2002. https://doi.org/10.1007/s00253-002-1076-7.
4. Badalyan SM, Zambonelli A. Biotechnological exploitation of macrofungi for the production of food, pharmaceuticals and cosmeceuticals. In: Sridhar KR, Deshmukh SK, editors. Advances in macrofungi: diversity, ecology and biotechnology. Boca Raton: CRC Press; 2019. p. 199–230.
5. Raja HA, Miller AN, Pearce CJ, Oberlies NH. Fungal identification using molecular tools: a primer for the natural products research community. J Nat Prod. 2017. https://doi.org/10.1021/acs.jnatprod.6b01085.
6. Motteu N, Goemaere B, Bladt S, Packeu A. Implementation of MALDI-TOF mass spectrometry to identify fungi from the indoor environment as an added value to the classical morphology-based identification tool. Front Allergy. 2022. https://doi.org/10.3389/falgy.2022.826148.
7. Li Y, Zhang J, Li T, Liu H, Li J, Wang Y. Geographical traceability of wild *Boletus edulis* based on data fusion of FT-MIR and ICP-AES coupled with data mining methods (SVM). Spectrochim Acta Part A Mol Biomol Spectrosc. 2017. https://doi.org/10.1016/j.saa.2017.01.029.
8. Li XP, Li J, Liu H, Wang YZ. A new analytical method for discrimination of species in Ganodermataceae mushrooms. Int J Food Prop. 2020. https://doi.org/10.1080/10942912.2020.1722159.
9. Edwards HGM, Russell NC, Weinstein R, Wynn-Williams DD. Fourier transform Raman spectroscopic study of fungi. J Raman Spectrosc. 1995;26:911–6.

Puliga *et al. Chem. Biol. Technol. Agric.*   (2022) 9:100

Page 9 of 10

10. Stöckel S, Kirchhoff J, Neugebauer U, Rösch P, Popp J. The application of Raman spectroscopy for the detection and identification of microorganisms. J Raman Spectrosc. 2016. https://doi.org/10.1002/jrs.4844.

11. Faghihzadeh F, Anaya NM, Schifman LA, Oyanedel-Craver V. Fourier transform infrared spectroscopy to assess molecular-level changes in microorganisms exposed to nanoparticles. Nanotechnol Environ Eng. 2016. https://doi.org/10.1007/s41204-016-0001-8.

12. Aroca RF. Plasmon enhanced spectroscopy. Phys Chem Chem Phys. 2013. https://doi.org/10.1039/c3cp44103b.

13. Aroca R. Surface-Enhanced Vibrational Spectroscopy. Chichester: Wiley; 2006.

14. Moskovits M. Surface-enhanced spectroscopy. Rev Mod Phys. 1985;57:783–826.

15. Moskovits M, Suh JS. Surface selection rules for surface-enhanced Raman spectroscopy: calculations and application to the surface-enhanced Raman spectrum of phthalazine on silver. J Phys Chem. 1984. https://doi.org/10.1021/j150667a013.

16. Butler HJ, Ashton L, Bird B, Cinque G, Curtis K, Dorney J, et al. Using Raman spectroscopy to characterize biological materials. Nat Protoc. 2016. https://doi.org/10.1038/nprot.2016.036.

17. Le Ru EC, Etchegoin PG. Principles of surface enhanced Raman spectroscopy (and related plasmonic effects). Amsterdam: Elsevier; 2009.

18. Lee HK, Lee YH, Koh CSL, Phan-Quang GC, Han X, Lay CL, et al. Designing surface-enhanced Raman scattering (SERS) platforms beyond hotspot engineering: emerging opportunities in analyte manipulations and hybrid materials. Chem Soc Rev. 2019. https://doi.org/10.1039/c7cs00786h.

19. Zhang Y, Zhao S, Zheng J, He L. Surface-enhanced Raman spectroscopy (SERS) combined techniques for high-performance detection and characterization. TrAC Trends Anal Chem. 2017. https://doi.org/10.1016/j.trac.2017.02.006.

20. Giannini V, Sánchez-Gil J, García-Ramos JV. Modelo teórico del mecanismo electromagnético en espectroscopia SERS. Óptica Pura y Apl. 2004;37:97–102.

21. Guerrini L, Izquierdo-Lorenzo I, Rodriguez-Oliveros R, Sanchez-Gil JA, Sanchez-Cortes S, Garcia-Ramos JV, et al. α, ω-aliphatic diamines as molecular linkers for engineering Ag nanoparticle clusters: tuning of the interparticle distance and sensing application. Plasmonics. 2010. https://doi.org/10.1007/s11468-010-9143-x.

22. Kneipp K, Flemming J. Surface enhanced Raman scattering (SERS) of nucleic acids adsorbed on colloidal silver particles. J Mol Struct. 1986. https://doi.org/10.1016/0022-2860(86)87041-7.

23. Barhoumi A, Halas NJ. Label-free detection of DNA hybridization using surface enhanced Raman spectroscopy. J Am Chem Soc. 2010. https://doi.org/10.1021/ja105678z.

24. Calderon I, Guerrini L, Alvarez-Puebla RA. Targets and tools: nucleic acids for surface-enhanced Raman spectroscopy. Biosensors. 2021. https://doi.org/10.3390/bios11070230.

25. Fazio B, D'Andrea C, Foti A, Messina E, Irrera A, Donato MG, et al. SERS detection of biomolecules at physiological pH via aggregation of gold nanorods mediated by optical forces and plasmonic heating. Sci Rep. 2016. https://doi.org/10.1038/srep26952.

26. Almehmadi LM, Curley SM, Tokranova NA, Tenenbaum SA, Lednev IK. Surface enhanced Raman spectroscopy for single molecule protein detection. Sci Rep. 2019. https://doi.org/10.1038/s41598-019-48650-y.

27. Han XX, Huang GG, Zhao B, Ozaki Y. Label-free highly sensitive detection of proteins in aqueous solutions using surface-enhanced Raman scattering. Anal Chem. 2009. https://doi.org/10.1021/ac900395x.

28. Wang K, Pu H, Sun DW. Emerging spectroscopic and spectral imaging techniques for the rapid detection of microorganisms: an overview. Compr Rev Food Sci Food Saf. 2018. https://doi.org/10.1111/1541-4337.12323.

29. Petersen M, Yu Z, Lu X. Application of Raman spectroscopic methods in food safety: a review. Biosensors. 2021. https://doi.org/10.3390/bios11060187.

30. Dina NE, Gherman AMR, Chiş V, Sârbu C, Wieser A, Bauer D, et al. Characterization of clinically relevant fungi via SERS fingerprinting assisted by novel chemometric models. Anal Chem. 2018. https://doi.org/10.1021/acs.analchem.7b03124.

31. Witkowska E, Jagielski T, Kamińska A, Kowalska A, Hryncewicz-Gwóźdź A, Waluk J. Detection and identification of human fungal pathogens using surface-enhanced Raman spectroscopy and principal component analysis. Anal Methods. 2016. https://doi.org/10.1039/c6ay02957d.

32. Prusinkiewicz MA, Farazkhorasani F, Dynes JJ, Wang J, Gough KM, Kaminskyj SGW. Proof-of-principle for SERS imaging of *Aspergillus nidulans* hyphae using in vivo synthesis of gold nanoparticles. Analyst. 2012. https://doi.org/10.1039/c2an35620a.

33. Lemma T, Wang J, Arstila K, Hytönen VP, Toppari JJ. Identifying yeasts using surface enhanced Raman spectroscopy. Spectrochim Acta Part A Mol Biomol Spectrosc. 2019. https://doi.org/10.1016/j.saa.2019.04.010.

34. Ramirez-Perez JC, Reis AT, Olivera CLP, Rizzutto MA. Impact of silver nanoparticles size on SERS for detection and identification of filamentous fungi. Spectrochim Acta Part A Mol Biomol Spectrosc. 2022. https://doi.org/10.1016/j.saa.2022.120980.

35. Yüksel S, Schwenkbier L, Pollok S, Weber K, Cialla-May D, Popp J. Label-free detection of *Phytophthora ramorum* using surface-enhanced Raman spectroscopy. Analyst. 2015. https://doi.org/10.1039/c5an01156f.

36. Royse DJ, Baars J, Tan Q. Current overview of mushroom production in the world. In: Zied DC, Pardo-Giménez A, editors. Edible and medicinal mushrooms: technology and applications. Chichester: John Wiley & Sons Ltd; 2017. p. 5–13.

37. Bijalwan A, Bahuguna K, Vasishth A, Singh A, Chaudhary S, Dongariyal A, et al. Growth performance of *Ganoderma lucidum* using billet method in Garhwal Himalaya India. Saudi J Biol Sci. 2021. https://doi.org/10.1016/j.sjbs.2021.03.030.

38. Zambonelli A, Iotti M, Puliga F, Hall IR. Enhancing white truffle (Tuber magnatum Picco and T borchii Vittad) cultivation through biotechnology innovation. In: Al-Khayri JM, Jain SM, Johnson DV, editors. Advances in plant breeding strategies: vegetable crops. Cham: Springer; 2021.

39. Fornito S, Puliga F, Leonardi P, Di Foggia M, Zambonelli A, Francioso O. Degradative ability of mushrooms cultivated on corn silage digestate. Molecules. 2020. https://doi.org/10.3390/molecules25133020.

40. Puliga F, Leonardi P, Minutella F, Zambonelli A, Francioso O. Valorization of hazelnut shells as growing substrate for edible and medicinal mushrooms. Horticulturae. 2022. https://doi.org/10.3390/horticulturae8030214.

41. Ma G, Yang W, Mariga AM, Fang Y, Ma N, Pei F, et al. Purification, characterization and antitumor activity of polysaccharides from *Pleurotus eryngii* residue. Carbohydr Polym. 2014. https://doi.org/10.1016/j.carbpol.2014.07.069.

42. Leopold N, Lendl B. A new method for fast preparation of highly surface-enhanced Raman scattering (SERS) active silver colloids at room temperature by reduction of silver nitrate with hydroxylamine hydrochloride. J Phys Chem B. 2003. https://doi.org/10.1021/jp027460u.

43. Zanasi G, Rubira RJG, Francioso O, Cañamares MV, Constantino CJL, Sanchez-Cortes S. Sensing atrazine herbicide degradation products through their interactions with humic substances by surface-enhanced Raman scattering. Chemosensors. 2021. https://doi.org/10.3390/chemosensors9060148.

44. Lin L, Xu J. Fungal pigments and their roles associated with human health. J Fungi. 2020. https://doi.org/10.3390/JOF6040280.

45. Gieroba B, Sroka-Bartnicka A, Kazimierczak P, Kalisz G, Lewalska-Graczyk A, Vivcharenko V, et al. Surface chemical and morphological analysis of chitosan/1,3-β-D-glucan polysaccharide films cross-linked at 90 °C. Int J Mol Sci. 2022. https://doi.org/10.3390/ijms23115953.

46. Otto C, van den Tweel TJJ, de Mul FFM, Greve J. Surface-enhanced Raman spectroscopy of DNA bases. J Raman Spectrosc. 1986. https://doi.org/10.1002/JRS.1250170311.

47. Xia ZK, Ma QH, Li SY, Zhang DQ, Cong L, Tian YL, et al. The antifungal effect of silver nanoparticles on *Trichosporon asahii*. J Microbiol Immunol Infect. 2016. https://doi.org/10.1016/J.JMII.2014.04.013.

48. Kim SW, Jung JH, Lamsal K, Kim YS, Min JS, Lee YS. Antifungal effects of silver nanoparticles (AgNPs) against various plant pathogenic fungi. Mycobiology. 2018. https://doi.org/10.5941/MYCO.2012.40.1.053.

49. Panáček A, Kolář M, Večeřová R, Prucek R, Soukupová J, Kryštof V, et al. Antifungal activity of silver nanoparticles against *Candida* spp. Biomaterials. 2009. https://doi.org/10.1016/J.BIOMATERIALS.2009.07.065.

50. Kim JS, Kuk E, Yu KN, Kim JH, Park SJ, Lee HJ, et al. Antimicrobial effects of silver nanoparticles. Nanomed Nanotech Biol Med. 2007. https://doi.org/10.1016/J.NANO.2006.12.001.

51. Dibrov P, Dzioba J, Gosink KK, Häse CC. Chemiosmotic mechanism of antimicrobial activity of Ag$^+$ in *Vibrio cholerae*. Antimicrob Agents Chemother. 2002. https://doi.org/10.1128/AAC.46.8.2668-2670.2002.
52. Kim J, Lee J, Kwon S, Jeong S. Preparation of biodegradable Polymer/ Silver nanoparticles composite and its antibacterial efficacy. J Nanosci Nanotechnol. 2009. https://doi.org/10.1166/JNN.2009.C096.
53. Rivas L, Murza A, Sánchez-Cortés S, García-Ramos JV. Interaction of antimalarial drug quinacrine with nucleic acids of variable sequence studied by spectroscopic methods. J Biomol Struct Dyn. 2000. https://doi.org/10.1080/07391102.2000.10506674.
54. Jurasekova Z, Garcia-Ramos JV, Domingo C, Sanchez-Cortes S. Surface-enhanced Raman scattering of flavonoids. J Raman Spectrosc. 2006. https://doi.org/10.1002/jrs.1634.
55. Martin-Sanchez PM, Sanchez-Cortes S, Lopez-Tobar E, Jurado V, Bastian F, Alabouvette C, et al. The nature of black stains in Lascaux Cave, France, as revealed by surface-enhanced Raman spectroscopy. J Raman Spectrosc. 2012. https://doi.org/10.1002/jrs.3053.
56. De La Rosa JM, Martin-Sanchez PM, Sanchez-Cortes S, Hermosin B, Knicker H, Saiz-Jimenez C. Structure of melanins from the fungi *Ochroconis lascauxensis* and *Ochroconis anomala* contaminating rock art in the Lascaux Cave. Sci Rep. 2017. https://doi.org/10.1038/s41598-017-13862-7.
57. Mirończuk-Chodakowska I, Witkowska AM. Evaluation of polish wild mushrooms as beta-glucan sources. Int J Environ Res Public Health. 2020. https://doi.org/10.3390/ijerph17197299.
58. Chen L, Xu W, Lin S, Cheung PCK. Cell wall structure of mushroom sclerotium (Pleurotus tuber-regium): part 1 fractionation and characterization of soluble cell wall polysaccharides. Food Hydrocoll. 2014. https://doi.org/10.1016/j.foodhyd.2013.09.023.
59. Gow NAR, Latge J-P, Munro CA. The fungal cell wall: structure, biosynthesis, and function. Microbiol Spectr. 2017. https://doi.org/10.1128/microbiolspec.FUNK-0035-2016.
60. Venturella G, Ferraro V, Cirlincione F, Gargano ML. Medicinal mushrooms: bioactive compounds, use, and clinical trials. Int J Mol Sci. 2021. https://doi.org/10.3390/ijms22020634.

Publisher's Note